1512–1521 *Nucleic Acids Research, 2002, Vol. 30, No. 7*

Receptor-mediated endocytosis of phosphodiester oligonucleotides in the HepG2 cell line: evidence for non-conventional intracellular trafficking

Philippe de Diesbach[1], Francisca N'Kuli[1], Catherine Berens[1,2], Etienne Sonveaux[2], Michel Monsigny[3], Annie-Claude Roche[3] and Pierre J. Courtoy[1,*]

[1]Cell Biology Unit, Christian de Duve Institute of Cellular Pathology and Université catholique de Louvain, UCL 7541, 75 Avenue Hippocrate, B-1200 Brussels, Belgium, [2]Laboratoire de Chimie Thérapeutique et de Radiopharmacie, Université catholique de Louvain, UCL 7340, 73 Avenue E. Mounier, B-1200 Brussels, Belgium and [3]Glycobiologie, Centre de Biophysique Moléculaire and Université d'Orléans, CNRS UPR 4301, rue Charles-Sadron, F-45071 Orléans Cedex 02, France

Received December 30, 2001; Revised and Accepted February 13, 2002

ABSTRACT

Having identified an oligonucleotide (ON) receptor in the HepG2 cell line, we have re-examined here the kinetics of ON uptake, subcellular distribution and intracellular localisation in these cells, at concentrations relevant for the study of a receptor-dependent process. Kinetic parameters of ON endocytosis were comparable with those of the receptor-mediated endocytosis tracer, transferrin (uptake equilibrium, saturation with concentration, specific competition and rapid efflux) and were clearly distinct from those of fluid-phase endocytosis. By analytical subcellular fractionation, particulate ON showed a bimodal distribution after 2 h of uptake, with a low-density peak superimposed on the distribution of endosomes, and a high-density peak overlapping lysosomes. After an overnight chase, only the high-density peak remained, but it could be dissociated from lysosomes, based on its refractoriness to displacement upon chloroquine-induced swelling. After 2 h of uptake at 300 nM ON-Alexa, a punctate pattern was resolved, by confocal microscopy, from those of transferrin, of a fluid-phase tracer, and of vital staining of lysosomes by LysoTracker. At 3 μM ON-Alexa, its pattern largely overlapped with the fluid-phase tracer and LysoTracker. Taken together, these data suggest that ON may be internalised at low concentrations by receptor-mediated endocytosis into unique endosomes, then to dense structures that are distinct from lysosomes. The nature of these two compartments and their significance for ON effect deserve further investigation.

INTRODUCTION

Oligonucleotides (ON) are short nucleic acid sequences with a large potential for research and clinical applications; one has already been approved for medical treatment and several others are currently in clinical trials (1). The original aim of using ON was an antisense effect (2), whereby specific binding to a targeted (pre)mRNA by Watson–Crick base pairing would sterically inhibit translation or induce recognition and degradation by RNases (3). However, several other ON-based approaches lead to a selective decrease in mRNA or protein content or function. They include the following: (i) ON designed to form a triple helix with a specific DNA sequence thereby blocking transcription (4); (ii) double stranded (ds) DNA decoy ON, which bind to selected transcription factors and prevent gene expression (5); (iii) RNA-ON (6) or DNA-ON (7) acting as ribozymes to directly degrade target mRNA; (iv) approaches exploiting the still poorly understood RNA interference, whereby double-stranded (ds)RNA, or fragments as small as 21 bp, can result in mRNA degradation (8); as a remarkable example, *Escherichia coli* expressing dsRNA produce specific RNA interference in the *Caenorhabditis elegans* larvae that feed on them (9); (v) secondary structure-based ON (aptamers) that interact either with proteins and inhibit their activity (10) or with RNA and compete for RNA-binding proteins, as is the case for the transactivation response element of HIV-1 (11). Remarkably, ON can also have 'positive' effects, such as correction of point mutations by homologous recombination (12) or the correction of splicing errors (e.g. in thalassemia; 13).

It has long been appreciated that biological applications of ON meet with two limitations: stability and accessibility. Non-modified ON are rapidly degraded by nucleases (14). Capping at the 5′-end, and particularly the 3′-end, protects ON against exonucleases (7,14). Backbone modifications yield additional ON protection, at the risk of compromising selectivity of interactions (13), but novel ON structures have been developed that combine improved stability and specificity (15). The second problem is accessibility. To exert their biological effect, ON must reach the cytosol and/or the nucleus. Nuclear pores are not a diffusion barrier, since ON micro-injected in the cytosol is almost immediately transferred into the nucleus (14,16,17). In contrast, the plasma membrane and the limiting membrane of endocytic organelles are impermeable to large polyanionic

*To whom correspondence should be addressed. Tel: +32 2 764 75 69; Fax: +32 2 764 75 43; Email: courtoy@cell.ucl.ac.be

molecules such as ON. Various physico-chemical methods (including liposome-mediated uptake, electroporation, micro-injection and permeabilisation using streptolysin-O) increase cytosolic penetration and are useful for research on cultured cells (reviewed in 18), but are not practical for *in vivo* studies or for therapy (1,3).

ON are spontaneously taken up by endocytosis, which can help reach their target (reviewed in 19). At high (micromolar) concentrations, ON are generally reported to be internalised by fluid-phase endocytosis, a process of too low efficiency to guarantee strictly specific effects (20–22). Indeed, high concentrations lead to multiple non-specific effects, some of which are even sequence dependent (23). In contrast, the most efficient mode of uptake of macromolecules is receptor-mediated endocytosis, whereby a plasma membrane protein binds a ligand and causes its clustering in clathrin-coated pits, resulting in accelerated internalisation. In this respect, ON was reported to bind as an 'opportunistic' ligand to the scavenger receptor in endothelial and Kupffer cells (~100 nM) (24) or to the integrin Mac-1 in polymorphonuclear leukocytes (~10 µM) (25), two carriers that lead to receptor-mediated endocytosis. ON uptake can also be enhanced by the conjugation to a specific ligand, as is the case in hepatocytes after derivatisation with galactosyl moieties (26). A variety of unidentified proteins, depending on the cell type studied, have also been suggested to act as specific 'receptors' for ON (20,21,27,28). One such ON-binding protein was found in lysates of the human HepG2 hepatoma cell line (29), where we have recently identified, by *in situ* photo-affinity labelling and ligand blotting, a membrane receptor that binds ON with a K_d of ~200 nM, and for which we reported a partial amino acid sequence as a novel protein (30).

After endocytosis, ON are sequestered in compartments of unknown nature (22,31,32), from which they are thought to escape by a still elusive and presumably inefficient mechanism. The rate of ON uptake and its fate vary with backbone and end modifications. Based on relief by monensin of fluorescence quenching, fluoresceinated ON phosphorothioates were reported to occur in acidic compartments, compatible with lysosomes (the usual end-compartment of endocytic sequestration), whereas organelles accumulating fluoresceinated ON phosphodiesters appeared not or poorly acidified, indicating differential intracellular routing (31). End modifications by signalling peptides may also reroute derivatised ON to different intracellular compartments (32).

In the present study, we have combined kinetic studies, subcellular fractionation and confocal microscopy to analyse the endocytic properties and fate of ON phosphodiesters protected at both ends in HepG2 cell line, by focusing on the low concentrations that should ensure receptor-specific uptake.

MATERIALS AND METHODS

Tracer source and modifications

We used two derivatives of a phosphodiester 25mer ON, with sequence complementarity to the AUG initiation site of HIV-1_{gag} (CTCTCGCACCCATCTCTCTCCTTCT) and protected by a 3′-end phosphoro-alkylamine (Eurogentec, Seraing, Belgium) (33). For biochemical studies, one derivative bearing a fluorescein moiety on its 5′-end was radioiodinated with IodoBeads (referred to as ^{125}I-ON) to a specific radioactivity of ~9.6×10^{16} Bq/mol (Pierce, Rockford, IL), as previously described (30,34). The second one, bearing a disulfide bridge on its 5′-end, was conjugated with fluorophores Alexa 488 (green signal) or Alexa 568 (red signal; both from Molecular Probes, Eugene, OR) by disulfide reduction followed by alkylation with a maleimide derivative of the fluorophore (adapted from ref. 34, yielding a molar ratio close to the unit). Similarly, iron-saturated transferrin (Sigma, St Louis, MO) was radioiodinated using IodoBeads (to 9×10^{14} Bq/mol), or conjugated to Alexa 568, using a Molecular Probes protein labelling kit, according to the manufacturer's instructions (with a molar ratio close to 2).

Horseradish peroxidase (HRP; type II) was from Roche Diagnostics (Brussels, Belgium). Alexa 568-labelled dextran (10 000 Da) and LysoTracker green were from Molecular Probes. Poly(C), poly(G) and poly(I), tRNA (purified from baker's yeast), ATPγ-S and GTPγ-S were from Sigma. Fraxiparine® was from Sanofi (Paris, France). The phosphorothioate SdC-28 (a 28 homo-cytidine polymer) was from the Pasteur Institute (Paris, France), and the phosphorothioate Gem91 (with the same sequence as the 25mer phosphodiester ON used) was a kind gift from Dr S. Agrawal (Hybridon, Worcester, MA).

Tracer uptake

HepG2 cell lines were obtained from the American Type Tissue Culture Collection, or received from Dr D. Hoekstra (Groningen, The Netherlands) or Dr G. Strous (Utrecht, The Netherlands), and propagated as described (30). For the experiments, cells were cultured in Petri dishes to near confluency (~3×10^6 in a 30 cm^2 dish) and incubated in serum-free RPMI, as previously described (30) at 37°C for 1 h with either 4 mg/ml HRP (100 µM), 5 µg/ml ^{125}I-transferrin (62 nM) or 1 µg/ml ^{125}I-fluorescein-ON (125 nM), unless otherwise specified. After uptake, dishes were transferred to 4°C and extensively washed (three times with PBS containing 0.44 mM Ca^{2+}, three times with PBS-Ca^{2+} supplemented with 1% BSA, and three times with PBS-Ca^{2+}, for 5 min each). This washing procedure proved essential to minimise non-specific surface binding. After surface digestion by 0.1% (w/v) pronase (Sigma) in RPMI medium for 1 h, cells were harvested by centrifugation, briefly rinsed twice with PBS and lysed in 0.01% (v/v) Triton X-100. To normalise between dishes, the protein content was quantified by the bicinchoninic acid (Sigma) procedure (3×10^6 HepG2 cells contain ~1 mg cell protein) (35). HRP was assayed by a colorimetric assay using orthodianisidine (Sigma) as substrate (36). Data analysis by non-linear regression was performed using graphpad software (www.graphpad.com).

Analytical subcellular fractionation

Cells (~30×10^6 in a 175 cm^2 dish) were incubated at 37°C for 2 h in RPMI medium without serum, supplemented with 125–250 nM ^{125}I-ON, either alone or combined with 100 µM HRP, then washed as above. For pulse-chase experiments, cells were similarly incubated for 2 h with ^{125}I-ON without serum, briefly washed five times with PBS then chased for 22 h in fresh medium supplemented with 10% serum (required to sustain overnight cell viability). For density-shift experiments, cells were further treated with 100 µM chloroquine (Sigma) for the last 4 h of the chase. Cells were washed, surface-digested

with pronase as above, and washed pellets were resuspended in 4 ml of the homogenisation medium SIE (0.25 M sucrose, 3 mM imidazole, 1 mM EDTA, pH 7.0).

Extraction and differential sedimentation into a low-speed pellet (the so-called nuclear fraction), a high-speed pellet (postnuclear particles) and a high-speed supernatant were performed as described (30). Postnuclear particles were resuspended in 2 ml of SIE. One millilitre was saved for further analysis and the other was loaded on the top of a 10.5 ml linear sucrose gradient in 3 mM imidazole, 1 mM EDTA, pH 7.0, ranging from 1.10 to 1.30 g/ml in density, over a 0.5 ml cushion (1.34 g/ml in density). After centrifugation at 20 000 r.p.m. for 18 h in a SW40 rotor (Beckman, Palo Alto, CA; 55×10^6 $g \times$ min), 12 fractions of ~1 ml were eluted from the bottom and their density was measured by refractometry. Cathepsin B was assayed by a fluorescent method based on the cleavage of α-*N*-benzoyl-DL-arginine-2-naphtylamide (Sigma) (37). Phosphodiesterase activity was assayed by a colorimetric method based on paranitrophenylthymidylate 5′-monophosphate hydrolysis (Sigma) (38). To compare and average density gradients, results were standardised according to Leighton *et al.* (39), and presented as density/frequency histograms.

Confocal microscopy

HepG2 cells were plated at ~3×10^4 cells/cm^2 and grown for 36 h in LabTek chambers (borosilicate coverglass, Nunc, Roskilde, Denmark) that were precoated with serum, rinsed for 30 min with serum-free medium and incubated at 37°C for 1–2 h with 300 nM ON-Alexa 488, followed by three washes in PBS-Ca^{2+} and one wash with PBS-Ca^{2+} containing 1% BSA, for 5 min each, at 4°C in the dark. To label cell contours, cells were further incubated for 1 h at 4°C in PBS-Ca^{2+} containing 1% BSA and 20 µg/ml rhodamine-labelled concanavalin A (Sigma), then washed again with PBS-Ca^{2+} containing 1% BSA and three times with PBS-Ca^{2+}, for 5 min each. For double uptake experiments, 300 nM ON-Alexa 488 or -Alexa 568 was combined with either 80 nM transferrin-Alexa 568, 50 µM dextran-Alexa 568 or 80 nM LysoTracker green, followed by the same washing procedure. For experiments with LysoTracker, this compound was also present in washing solutions. Cells were immediately examined (without surface digestion) in their living state with an Axiovert confocal microscope (Zeiss, Oberkochen, Germany), coupled to a MRC1024 confocal scanning laser equipment (Bio-Rad, Richmond, CA).

RESULTS

Quantitative evidence for ^{125}I-ON receptor-mediated endocytosis in the HepG2 cell line

Two criteria for endocytosis are (i) dependence of temperature (arrest at 4°C) and (ii) acquisition of resistance to surface digestion. In order to establish a biochemical assay for receptor-dependent ON endocytosis in the HepG2 cell line, we first evaluated the possibility of removing ^{125}I-ON bound at 4°C to the plasma membrane, while preserving tracer internalised at 37°C. For this purpose, cells were post-treated at 4°C by pronase (40). Incubation with ^{125}I-ON was performed at 125 nM, close to the K_d of its putative receptor (30) and, as previously, in serum-free medium to prevent ON binding to albumin (41). To compare modes of entry, cells were incubated in parallel with 62 nM ^{125}I-transferrin or 100 µM HRP, two classical tracers of receptor-mediated and fluid-phase endocytosis, respectively. After uptake at 37°C for 1 h, followed by extensive washing and surface-protease digestion at 4°C, 836 ± 62 fmol ^{125}I-ON, 2688 ± 252 fmol ^{125}I-transferrin and 8375 ± 2012 fmol HRP, based on enzymatic activity (means ± SEM; n = 15, 6 and 6, respectively) were found to be associated per mg cell protein. These values were highly consistent within a given experiment but showed significant variations between experiments. Uptake was severely inhibited at 4°C for ON and HRP (>80%) and essentially abolished for transferrin (>97%). This suggested that ON or ON–receptor complexes were transferred at 37°C into a compartment resistant to surface digestion, compatible with endocytosis into intracellular structures, a conclusion directly confirmed by morphological evidence using fluorescent ON (see Fig. 6A). The selectivity of receptor-mediated endocytosis is evidenced by the ratio of intracellular versus extracellular tracer concentrations (endocytosis uptake efficiency). After 1 h of uptake at 37°C, these ratios were ~80-fold higher for 125 nM ^{125}I-ON (1.34) and 520-fold higher for 62 nM ^{125}I-transferrin (8.67) than for 100 µM HRP (0.017). These observations are in good agreement with the well-known efficacy of receptor-mediated endocytosis of transferrin, and are compatible with a similar mechanism operating for ^{125}I-ON capture into the HepG2 cell line.

The kinetics of accumulation and efflux of tracers shown at Figure 1 also reflects their mode of endocytosis. The increase of peroxidase activity (indicating HRP accumulation) was linear, as predicted for continuous filling of the late endocytic apparatus by fluid-phase endocytosis (Fig. 1C). In contrast, accumulation of ^{125}I-ON (Fig. 1A) and ^{125}I-transferrin (Fig. 1B) that were not released by surface pronase treatment levelled off after 1–2 h, compatible with saturation of an intracellular compartment in equilibrium with the cell surface pool. As compared with HRP uptake, the initial rate of endocytosis derived from curve fitting was 150-fold faster for ON and 1900-fold faster for transferrin. Whereas loss of peroxidase activity (indicating HRP efflux; Fig. 1F) was slow ($t_{½}$ of 17 min) and limited (~28% of release after 2 h of pulse), reflecting sequestration in late endosomes and lysosomes (HRP activity resists lysosomal proteolysis for several hours), the efflux of ^{125}I-transferrin (Fig. 1E) was more rapid ($t_{½}$ of 10 min) and almost complete (88% of release after 2 h), as expected; the efflux of ^{125}I-ON (Fig. 1G) was also rapid ($t_{½}$ of 11 min), but partial (~45% of release after 2 h of pulse). Upon longer chase intervals, regurgitation was clearly bi-exponential (with a $t_{½}$ ~10 h for the second component; data not shown).

Specificity of ^{125}I-receptor-mediated endocytosis in HepG2 cell line

Two additional hallmarks of receptor-mediated endocytosis are (i) saturation of uptake at high ligand concentration and (ii) specific competition for uptake by a large excess of the same or other ligand(s) for the same receptor, but not by non-cognate, yet structurally related compounds. When uptake was analysed at increasing ^{125}I-ON concentrations (Fig. 2A), two components could be distinguished that were better evidenced after logarithmic transformation of the endocytic uptake efficiency (Fig. 2B). A saturable component prevailed below 1 µM and a component of lower affinity accounted for additional uptake

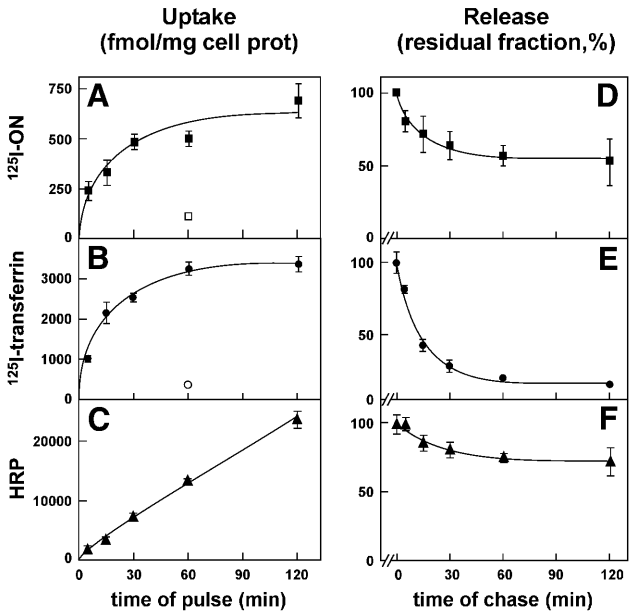

Figure 1. Comparison of the kinetics of ^{125}I-ON endocytosis and efflux with those of receptor-mediated and fluid-phase endocytic tracers. HepG2 cells were incubated at 37°C for the indicated times of pulse (**A**–**C**) or for 1 h (**D**–**F**) with 1 ml serum-free medium supplemented with either 125 nM ^{125}I-ON (A and D), 62 nM ^{125}I-transferrin (B and E), or 100 µM HRP (C and F) prior to washing and surface-protease digestion at 4°C, either without (A–C) or after chase in tracer-free medium for the indicated times (D–F). Pronase-resistant values (representing 30–50% of total cell-associated radioactivity for ^{125}I-ON, ~55% for ^{125}I-transferrin and essentially all cell-associated HRP activity) were normalised to the cell protein content in the lysate of each dish. These ratios are represented in A–C in absolute amounts and in D–F as a residual fraction, expressed as percentages of level at time 0 of chase. These experiments were reproduced two or three times and yielded comparable kinetics. Data shown are from a representative experiment and are means ± SD of three dishes. Curves were drawn after (i) non-linear fitting (A and B) based on the hyperbola $U = U_{max} \times x / (K_u + x)$, where U is actual uptake at a given time; U_{max} is the steady state accumulation, corresponding to 686 and 3367 fmol/mg cell protein, respectively, K_u is the half-time for saturation of uptake (15 and 13 min, respectively) and x is the actual time (min); (ii) linear regression (C); or (iii) non-linear fitting to a mono-exponential decay (D–F; for parameters, see Results).

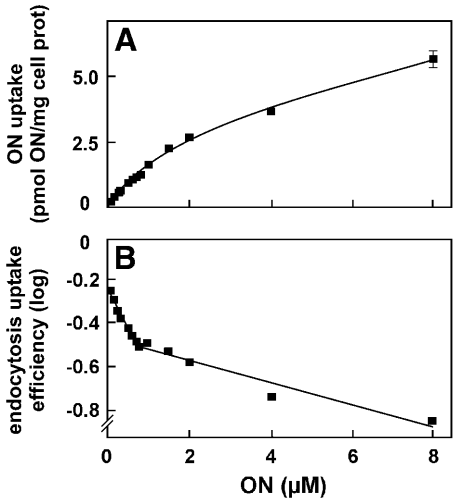

Figure 2. Saturation of ^{125}I-ON endocytosis. HepG2 cells were incubated at 37°C for 1 h with the indicated ^{125}I-ON concentrations. Protease-resistant radioactivity was measured as in Figure 1 and is presented as absolute values (**A**) or after logarithmic transformation (**B**) of endocytic uptake efficiency, both as a function of extracellular concentration. Data shown are means ± SD of three dishes. All but one error bar are included in the symbols. Curve A was fitted according to the two-hyperbolic model: $U = U_{max\ HA} \times x / (K_{U\ HA} + x) + U_{max\ LA} \times x / (K_{u\ LA} + x)$, where U is the actual uptake at a given concentration, $U_{max\ HA}$ and $U_{max\ LA}$ are saturation of uptake by high-affinity and low-affinity sites, respectively, $K_{U\ HA}$ and $K_{U\ LA}$ are corresponding half-saturation concentrations, and x is the actual extracellular concentration. To decrease the confidence interval, the $K_{U\ HA}$ value was set at 220 nM, as measured in de Diesbach *et al.* (30). Deduced parameters were 0.48 pmol/mg protein for $U_{max\ HA}$, 9.68 pmol/mg protein for $U_{max\ LA}$ and 7.5 µM for $K_{U\ LA}$. This type of experiment was reproduced twice, yielding similar results.

above this concentration, both contributing equally around 1 µM. These two components are compatible with two different modes of endocytosis, namely receptor-mediated endocytosis at low ON concentrations, and non-specific endocytosis accounting for additional accumulation at high concentrations. However, the efficiency of the latter process (0.14) still exceeded by approximately one order of magnitude that of fluid-phase endocytosis (0.017; see above), thus pointing to non-specific adsorptive endocytosis.

Specificity of uptake was addressed by competition experiments (Fig. 3). As illustrated in Figure 3A, all oligonucleotides tested efficiently competed for tracer ^{125}I-ON uptake: the phosphorothioate Gem91 was the strongest competitor (Ki, ~10 nM), followed by SdC28 (a phosphorothioate homopolymer) and Poly(I) (a mixture of phosphodiester homopolymers of various length, Ki ~30 nM for both). Poly(G) and poly(C) were 2.5- and 4.4-fold less potent (Fig. 3B). The efficient competition by several non-modified ONs ruled out the possibility of a predominant binding of ^{125}I-ON via its labelling moiety. In contrast, neither the non-hydrolysable mononucleotides ATPγ-S and GTPγ-S nor the non-nucleotidic sulphated polyanion, Fraxiparine®, a heparan sulphate fraction of comparable mass and charge to that of ON, significantly interfered with ^{125}I-ON uptake (Fig. 3B). Noticeably, a mixture of tRNAs, known for their secondary structures, were good competitors up to 100 nM, but failed to further interfere with ON uptake above this concentration, suggesting that at least two classes of ON-binding proteins are involved. For control, none of these treatments significantly interfered with receptor-mediated endocytosis of transferrin and with fluid-phase endocytosis of peroxidase (data not shown). Thus, the receptor(s) involved appeared to recognise oligo(deoxy)ribonucleotides with a high specificity. To address the fate of ON that had been taken up at low concentrations presumably by receptor-mediated endocytosis, we next resorted to subcellular fractionation combined with confocal microscopy.

Analytical subcellular fractionation

To compare the distribution of ON that was not released by surface pronase treatment with those of endogenous marker enzymes as well as of the established endocytic tracers, ^{125}I-transferrin and HRP, cells were incubated with low concentrations (125–250 nM) of ^{125}I-ON for 2 h, with or without a 22 h chase. To further test for association with lysosomes, the equilibrium density of these organelles was shifted by a 4 h incubation in the presence of 100 µM chloroquine prior to cell collection. In preliminary experiments, ^{125}I-ON

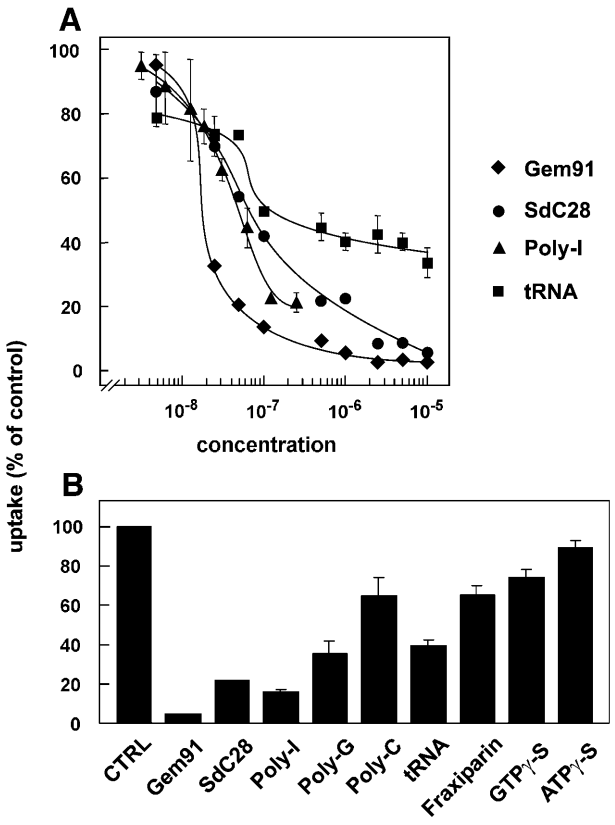

Figure 3. Specificity of ^{125}I-ON endocytosis. HepG2 cells were incubated at 37°C for 1 h with 15 nM ^{125}I-ON together with the indicated concentrations of competitors (**A**), or with 1.5 μM of the indicated competitors (**B**). Values are expressed as percentages of protease-resistant radioactivity in the absence of competitors and are the means ± SD of three dishes. Where non visible, error bars are included in the symbols. For each competitor, similar results were reproduced in at least one other experiment.

integrity was assessed by 15% SDS–PAGE; this analysis showed that, after surface pronase digestion, >90% of cell-associated ^{125}I-ON was intact after a 2 h pulse and >50% after 2 h pulse/22 h chase (data not shown). This surprisingly high fractional integrity after prolonged cell incubation provides a first indication against its retention in nuclease-rich compartments such as lysosomes.

Overall, the homogenisation procedure was (i) efficient, since ~80% of the lysosomal marker, cathepsin B, and >90% of the plasma/endosomal membranes marker, alkaline phosphodiesterase I, were extracted in the post-nuclear supernatant; and (ii) not harmful, since 70–90% of the extracted markers were sedimentable in the high-speed pellet, which amounted to ~40% of total cell protein. Upon chloroquine treatment, cell-associated cathepsin B activity was decreased by 3.2 ± 0.7-fold (mean ± SD; $n = 3$), in good agreement with the literature (42). A higher and variable proportion of total cell cathepsin B was recovered in the high-speed supernatant, reflecting vulnerability of swollen lysosomes. At the opposite of the cathepsin B content, the ON accumulation was not appreciably altered by chloroquine (105% of control; $n = 2$). About one-third of ON remained in the low-speed pellet and about two-thirds of extracted ON was sedimentable in the post-nuclear particles, both in untreated and chloroquine-treated cells. Unequal sedimentability of cathepsin B and ON in the post-nuclear supernatants of individual fractionation experiments provided a second argument against a major association of ON with lysosomes. To exclude a nuclear relocation artefacts due to release from broken organelles and selective uptake by the nuclei (16,17), a homogenate of naive, pronase-treated cells was incubated at 4°C for 1 h with ^{125}I-ON before the fractionation procedure; 97% of the ON was found in the high-speed supernatant (cytosolic) fraction and only 1% in the low-speed pellet (nuclear) fraction. This *in vitro* mixing experiment excludes the fact that ON occurring in the low-speed pellet would result from artificial nuclear transfer after homogenisation. However, it does not allow the conclusion that the ON occurring in the low-speed pellet after ON endocytosis necessarily reflects genuine nuclear location.

Next, post-nuclear particles were analysed by equilibration after top loading on linear sucrose gradients (Fig. 4). After 2 h of uptake, the density distribution of ^{125}I-ON was bimodal, with a low-density peak at 1.12 g/ml and a high-density peak of comparable size at 1.21 g/ml (Fig. 4A), and clearly distinct from the overall protein distribution (Fig. 4D). To further exclude ^{125}I-ON re-absorption to organelle membranes, a post-nuclear pellet obtained from naive cells was again mixed *in vitro* with ^{125}I-ON and equilibrated in parallel: all radioactivity remained in the loading zone, at the top of the gradient. In a second control, postnuclear particles of cells incubated with ^{125}I-ON were loaded below the gradient and allowed to float into the gradient: the same bimodal pattern, with identical density peaks, was observed as after loading on the top of the gradient, demonstrating that equilibrium density was reached in both cases (data not shown). In contrast to ON, HRP taken up by the same cells showed a clearly unimodal peak of activity at 1.12 g/ml (Fig. 4B), closely coinciding with the plasma/endosomal membranes marker, alkaline phosphodiesterase I (Fig. 4C), and with the low-density peak of ON. The high-density peak of ON partially overlapped with that of the lysosomal marker, cathepsin B (see Fig. 5B). This analysis was thus compatible with a dual localisation of ^{125}I-ON, partially endosomal and partially dense, possibly in a lysosomal subset.

To further test for lysosomal accessibility, ^{125}I-ON and HRP accumulation were followed by an overnight chase, to allow both tracers to progress along the endocytic apparatus (Fig. 5A). This extended chase decreased the cell ON content by ~90% (see above). The density distribution of the cell-associated radioactivity became essentially restricted to its dense component (1.19 g/ml; Fig. 5A) and largely overlapped the cathepsin B peak (1.18 g/ml; Fig. 5B, thin line), like peroxidase activity (Fig. 5C, thin line).

To directly address whether ON had actually reached lysosomes, cells were treated with chloroquine. This amphiphilic weak-base passes through biological membranes in its non-protonated form and becomes charged and trapped in closed acidified compartments (43). It is well established that acidotropic accumulation of chloroquine leads to a considerable concentration of the drug in lysosomes, in proportion to their transmembrane pH gradient. The resulting osmotic swelling of lysosomes provokes a selective shift of their equilibrium density (44). Whereas, upon chloroquine treatment, distributions of both the endogenous lysosomal marker, cathepsin B, and the exogenous tracer, HRP, having accumulated in lysosomes after a long chase, were clearly displaced towards lighter densities

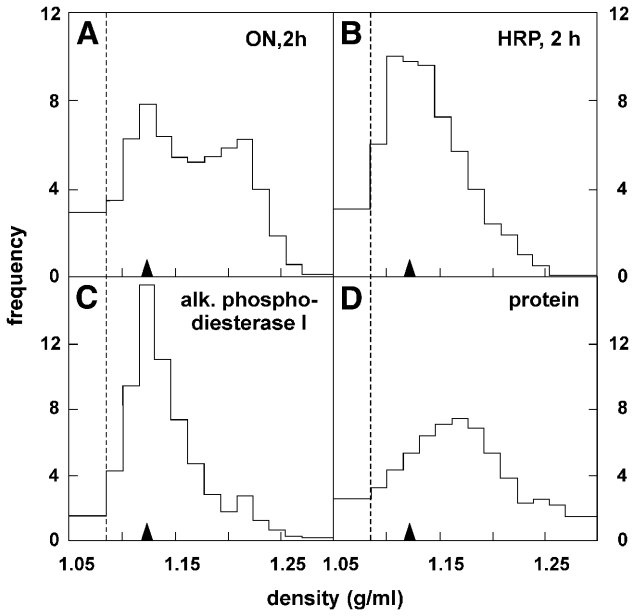

Figure 4. Density distribution after ^{125}I-ON pulse. HepG2 cells were incubated at 37°C for 2 h with either 125–250 nM ^{125}I-ON (**A**) or 100 µM HRP (**B**), washed and surface digested with pronase at 4°C. After homogenisation, postnuclear particles were loaded on the top of linear sucrose density gradients (loading zone is left of the dotted line) and centrifuged to equilibrium. Distributions were normalised as density/frequency histograms. Data shown are averages of three fractionation experiments and compared with the distribution of the plasma membrane/endosomal marker, alkaline phosphodiesterase I (**C**), and of total particulate protein (**D**). Recoveries ranged between 89 and 114%. For convenience, the position of ON low-density peak (1.13 g/ml in density; filled arrowheads) is repeated on each distribution.

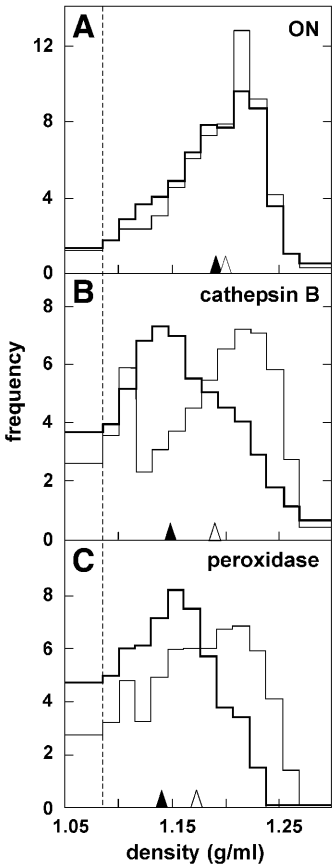

Figure 5. Dissociation between organelles containing ^{125}I-ON and lysosomes in sucrose gradients after pulse-chase. HepG2 cells were incubated at 37°C for 2 h with 250 nM ^{125}I-ON combined with 100 µM HRP in serum-free medium as in Figure 4, followed by a 22 h chase in the presence of serum. During the last 4 h, 100 µM chloroquine was added (thick line) or not (thin line), prior to washing and pronase digestion. Distributions of ^{125}I-ON (**A**), cathepsin B (**B**) and HRP activities (**C**) are compared in the same cells and presented as in Figure 4. Recoveries ranged between 82 and 123%. Data are from a representative experiment out of three. Arrowheads represent median densities in the absence (open symbols) and presence (filled symbols) of chloroquine.

(peaking at 1.13 g/ml; Fig. 5B and C, thick lines; compare open arrowheads with filled arrowheads), the ^{125}I-ON distribution in the same cells was not affected by the drug (Fig. 5A), thus being clearly resolved from the two lysosomal constituents. This dissociation strongly suggests that ^{125}I-ON internalised at low concentrations does not become appreciably associated with lysosomes. The resistance to chloroquine-induced displacement further indicates that the compartment containing phosphodiester ON is not actively acidified.

Confocal microscopy

We next attempted to localise, by confocal microscopy in living cells, fluorescent ON that had been taken up at concentrations relevant to study a receptor-mediated process. Although at 3 µM fluorescein-labelled ON was clearly evidenced in punctate intracellular structures, no signal was detected at 300 nM. Since it was uncertain whether the former signal reflected receptor-mediated endocytosis (see above), two other conjugates were prepared to exploit the higher fluorescence quantum yield of Alexa probes. Using these compounds, a detectable signal was clearly observed in discrete structures after ≥15 min incubation with 300 nM ON, when conjugated to either Alexa 488 (green) or Alexa 568 (red). Since these structures were frequently found near to the cell periphery, it was necessary for assessing endocytosis to delineate cell contours, for which we resorted to subsequent plasma membrane labelling at 4°C with a fluorescent lectin, rhodamine-labelled concanavalin A (Fig. 6A, red). This double labelling procedure demonstrated intracellular localisation of ON-Alexa 488. The specificity of uptake of ON-Alexa 488 was established, upon competition by a 100-fold excess of Gem91, by its complete disappearance at the appropriate confocal setting (Fig. 6B). This setting was thus selected for, and repeatedly validated by, subsequent experiments. The nature of the intracellular ON compartment was analysed by reference to endosomes, labelled upon receptor-mediated endocytosis of fluorescent transferrin, and to lysosomes, labelled by LysoTracker, a fluorescent acidotropic tracer that accumulates in lysosomes similarly to chloroquine. The specificity of the detection of transferrin-Alexa 568, after uptake by receptor-mediated endocytosis at 80 nM, was established by the total disappearance of intracellular signal upon competition with a 200-fold molar excess of unlabelled transferrin (Fig. 6D). High transferrin concentration did not detectably affect ON uptake (persistence of green signal in Fig. 6D), nor did high ON concentration affect intracellular transferrin signal (data not shown). Upon simultaneous incubation with 300 nM ON-Alexa 488 (green) and 80 nM transferrin-Alexa

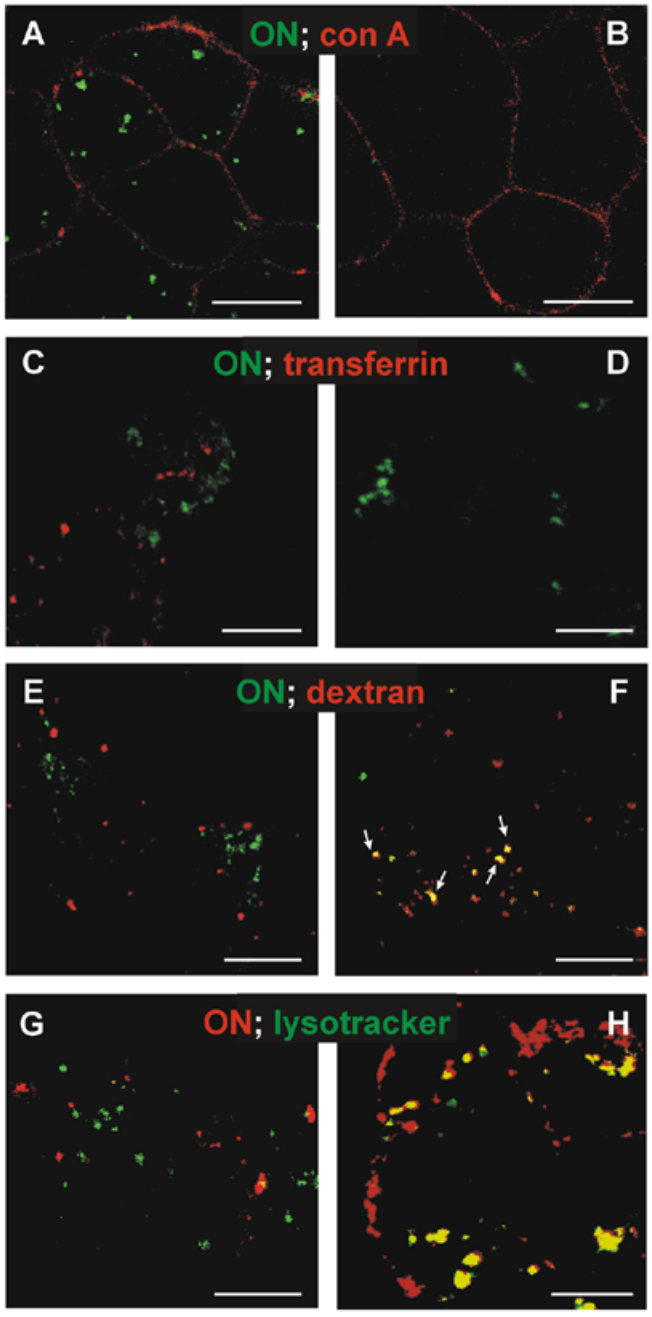

Figure 6. Confocal microscopy. (**A** and **B**) Specificity of intracellular ON labelling. HepG2 cells were grown in LabTek chambers and incubated at 37°C for 1 h with 300 nM ON-Alexa 488 (green), either alone (A) or combined with 30 µM Gem91 (B). After washing and labelling of cell contours with concanavalin A-rhodamine (red) at 4°C, cells were immediately analysed by confocal microscopy. (**C** and **D**) Comparison with transferrin-containing endosomes. Cells were incubated at 37°C for 1 h with 300 nM ON-Alexa 488 (green) together with 80 nM transferrin-Alexa 568 (red), either alone (C) or with an excess (1.6 µM) of unlabelled transferrin (D), extensively washed at 4°C and immediately examined. (**E** and **F**) Comparison with fluid-phase endocytosis. Cells were incubated at 37°C for 1 h with ON-Alexa 488 (green) at either 300 nM (E) or 3 µM (F), together with 50 µM dextran-Alexa 568 (fluid-phase tracer, red), washed and immediately examined. (**G** and **H**) Comparison with lysosomes. Cells were incubated at 37°C for 6 h with ON-Alexa 568 (red) at either 300 nM (G) or 3 µM (H), combined with the lysosomal vital stain LysoTracker (green) at 80 nM, washed and immediately examined. Bars indicate 10 µm.

568 (red) for 15 min (data not shown) or 2 h (Fig. 6C), transferrin appeared to reach multiple organelles dispersed among the entire cell cytoplasm, whereas ON remained predominantly in a peripheral cytoplasmic location. When both signals were merged, no co-localisation was detected (Fig. 6C), pointing to distinct endocytic pathways and, possibly, mechanisms.

As stated above, intracellular labelling of fluorescent ON reported in the literature had been obtained at higher concentrations (up to 7.5 µM) (23,31,32,45) that could reflect, at least in part, fluid-phase endocytosis. It was, therefore, essential to examine whether the intracellular route of ON would be different, depending on the mode of entry. Indeed, fluid-phase and adsorptive endocytic tracers become generally trapped in lysosomes whereas receptor-bound tracers may be targeted to various distinct compartments. For this purpose, we followed the fate of ON-Alexa 488 at 300 nM (to track receptor-mediated endocytosis), or at 3 µM (to also follow non-specific endocytosis); the ON signal was further compared with that of a fluorescent dextran, a well-established tracer of fluid-phase endocytosis (46). After 1 h of uptake at 300 nM, ON-Alexa 488 (green) was completely separated from dextran-Alexa 568 (Fig. 6E, red), but some co-localisation was evident at 3 µM ON-Alexa 488 (Fig. 6F, arrows).

Dissociation of the ON compartment from lysosomes was also tested by confocal microscopy, using lysosomal vital staining by LysoTracker green. The high acidotropic concentration of this compound, endowed with a low intrinsic fluorescence, generates a fluorescent signal specifically in these organelles (47). As expected, LysoTracker green essentially produced a perinuclear punctate pattern. When cells were incubated simultaneously with 300 nM ON-Alexa 568 (red) and LysoTracker (green), no co-localisation was detected between these two probes (Fig. 6G), whereas some co-localisation could be detected at 3 µM ON-Alexa 568 (Fig. 6H).

DISCUSSION

In this paper, we show that phosphodiester oligonucleotides, when taken up by the HepG2 cell line at low concentrations, are internalised by receptor-mediated endocytosis, transferred into low-density organelles that are distinct from transferrin-containing endosomes and stored in dense organelles that are distinct from lysosomes.

When applied at a concentration close to the K_d of the 66 kDa receptor recently identified by *in situ* photo-affinity labelling in the same cell line, the endocytic behaviour of ON completely differs from that of the fluid-phase tracer, HRP, and resembles that of the receptor-mediated endocytic tracer, transferrin. The initial clearance rate of ^{125}I-ON internalisation is ~2 log higher than for HRP, excluding fluid-phase endocytosis, but is similar to that of transferrin, which is internalised via clathrin-coated pits. Moreover, the endocytic constant (i.e. the ratio of intracellular over surface-bound values) (48), which best describes the rate of internalisation of membrane-associated constituents, can be estimated on the basis of the initial slope at 7% × min^{-1} for ON, as compared with 18% × min^{-1} for transferrin. Since transferrin receptors are concentrated ~10-fold in clathrin-coated pits (49), this suggests that ON–receptor complexes can also be concentrated, ~4-fold, in these structures. Overall, the hyperbolic internalisation kinetics and the considerable release of ON also

completely differ from the linear accumulation and marginal release of the fluid-phase tracer, HRP, and resemble those of transferrin. This suggests that a large fraction of ON/receptor complexes would rapidly recycle to the cell surface, together with ligands released into the extracellular medium, and that the plateau of uptake would reflect saturation of the specific cell endocytic machinery, when all accessible compartments containing cycling receptors have been reached (45).

Upon increasing ON concentration, surface receptors become saturated. Non-linear curve fitting allows one to distinguish two components: a saturable, high-affinity component, and an almost linear component above 1 μM. The endocytic efficiency of this linear component is, however, 10-fold higher than accounted for by fluid-phase endocytosis and therefore implies adsorptive non-specific endocytosis. At variance, the efficacy of ON endocytosis above 1 μM in L929 mouse fibroblast and in K562 human leukemia cell lines has been reported to be comparable with those of polyvinyl-pyrrolidone or sucrose, used to follow fluid-phase endocytosis (20,21). However, the endocytic uptake efficiency calculated from these two reports was much higher (>30-fold) than for HRP endocytosis in our experimental system. This discrepancy may be related, among other factors, to the difficulty in achieving complete removal of extracellular fluid-phase tracers by washing alone, which can be circumvented by cell surface digestion as used in the present study.

After ^{125}I-ON exposure at 4°C, protease treatment of washed cells releases ~90% of cell-associated radioactivity, while this value falls to ~50% after 1 h incubation at 37°C. Since it was ascertained that the integrity of ON was unaffected by the pronase solution, excluding significant contamination by a nuclease, the almost complete release of surface-bound ON after uptake at 4°C strongly suggests that ON receptors leading to efficient ON internalisation are proteic in nature. Partial resistance to pronase digestion after incubation at 37°C has been reported by other investigators (40) and indicates transfer of surface-bound ON to intracellular organelles. This was directly demonstrated by confocal microscopy.

The nature of ON receptors in the HepG2 cell line has been previously addressed by using *in situ* photo-affinity labelling of intact cells, as well as ligand blotting of cell lysates (30). Among various ON-binding bands, one protein candidate was singled out as an ON endocytic membrane receptor, based on its resistance to carbonate extraction and its partial sensitivity to cell-surface pronase digestion. By *in situ* photo-affinity labelling and ligand blotting, ^{125}I-ON binding was sensitive to competition by ON (C. Berens, unpublished results), but not by non-nucleotidic polyanions, arguing against non-specific electrostatic interaction (20,27). In the present report, a polysulphated polymer of comparable size (the small molecular weight heparin fragments, Fraxiparine®) failed to compete with the interaction. In contrast, all oligo- and polynucleotides tested, irrespective of the sugar residue and of the backbone (PO versus PS), were effective competitors indicating that we were dealing with an oligo- or polynucleotide receptor. The occurrence of a membrane receptor that recognises tRNA may be related to the recent demonstration of its transfer across the mitochondrial membrane in mammalian cells (50).

The nature of the ON-containing compartments was addressed by kinetic, fractionation and confocal studies. The existence of two components is indicated by a biphasic efflux kinetic (31), and by a bimodal distribution after subcellular fractionation. Available information does not allow the exclusion of a model involving two parallel pathways of different kinetics (i.e., a compartment rapidly accessible to endocytosis and recycling, corresponding to the low-density peak, and an unrelated slowly accessible compartment, corresponding to the high-density peak). However, a sequential model is more in agreement with the general knowledge of the endocytic apparatus.

Neither of these compartments appears to be actively acidified since ON internalised for up to 6 h failed to co-localise with LysoTracker by confocal microscopy and, after an overnight chase, failed to be shifted by chloroquine, in contrast to the lysosomal marker, cathepsin B, and the sequestered fluid-phase endocytic tracer, HRP. This contrasts with the acidification of phosphorothioate ON-containing compartment (31), indicating that the cargo could modify the fate of the ON receptor. These results are apparently in agreement with the reported absence of relief by monensin of acidic fluorescence quenching of fluoresceinated PO-ON internalised at micromolar concentrations in intact cells (31). However, when using the same micromolar concentrations, we found that some ON was clearly associated in LysoTracker-labelled structures located deep in the cell. Nevertheless, the bulk of ON remained at the cell periphery in structures devoid of detectable LysoTracker labelling. Such a heterogeneity emphasizes the complementary value of morphological approaches.

The identification of the two intracellular compartments involved in phosphodiester ON trafficking after incubation at sub-micromolar concentrations remains unclear and could in principle be addressed by immunolocalisation in confocal microscopy. However, contrary to ON derivatised with lysine-containing peptides (32), we found that ON used in this study were poorly cross-linked by aldehyde fixatives and serious artefacts in their localisation after non-aldehyde-based fixation have been reported (51). Although working on living cells is not very practical, because of the rapid ON efflux, this approach appears more reliable but precludes comparison with the immunolocalisation pattern of organelle markers.

As a final word of caution, it should be stressed that results reported in this paper on the uptake and subcellular fate of ON deal with an established cell line and an end-protected phophodiester ON. Whether they are applicable to other established cell lines, to cells in primary culture, or in living animals, and their relevance to other types of ON await to be ascertained. First, gene expression in established cell lines frequently differs from their *in situ* counterpart and their pattern is subject to drift with time. Cryptic viral or mycoplasma contamination, which could alter cellular uptake and intracellular routing, is also hard to totally exclude. Second, phosphorothioate ON, which are usually better inhibitors of gene expression than phosphodiesters, may interact with other receptors and/or follow other intracellular routes (31). Third, the peculiar endocytotic properties described in this report do not address the passage of ON across a membrane into the cytosolic compartment. Further investigations addressing these specific issues and concerns are clearly warranted.

ACKNOWLEDGEMENTS

We thank Dr U. Asseline (CNRS) and Mr Y. Aubert (INSERM) for their advice in ON synthesis and Dr S. Agrawal for providing Gem91. The assistance of Y. Marchand (typing) and M. Leruth (illustrations) are greatly appreciated. P.d.D. is a research fellow (SmithKline Beecham grant) of the Fonds National de la Recherche Scientifique (FNRS, Belgium). C.B. was a research fellow at the FNRS, then a recipient of a PhD training grant from UCL. This work was supported by grants to M.M., A.-C.R. and P.J.C. from the Agence Nationale de Recherche contre le SIDA (ANRS, France) as well as from FNRS, Concerted Research Actions and Interuniversity Attraction Poles (Belgium) to P.J.C.

REFERENCES

1. Rudin,C.M., Holmlund,J., Fleming,G.F., Mani,S., Stadler,W.M., Schuman,P., Monia,B.P., Johnston,J.F., Geary,R., Yu,R.Z., Kwoh,J., Dorr,F.A. and Ratain,M.J. (2001) Phase I trial of ISIS 5132, an antisense oligonucleotide inhibitor of c-raf-1, administered by 24-hour weekly infusion to patients with advanced cancer. *Clin. Cancer Res.*, **7**, 1214–1220.
2. Zamecnik,P.C. and Stephenson,M.L. (1978) Inhibition of Rous sarcoma virus replication and cell transformation by a specific oligodeoxynucleotide. *Proc. Natl Acad. Sci. USA*, **75**, 280–284.
3. Yu,R.Z., Zhang,H., Geary,R.S., Graham,M., Masarjian,L., Lemonidis,K., Crooke,R., Dean,N.M. and Levin,A.A. (2001) Pharmacokinetics and pharmacodynamics of an antisense phosphorothioate oligonucleotide targeting Fas mRNA in mice. *J. Pharm. Exp. Ther.*, **296**, 388–395.
4. Kukreti,S., Sun,J.-S., Garestier,T. and Hélène,C. (1997) Extension of the range of DNA sequences available for triple helix formation: stabilization of mismatched triplexes by acridine-containing oligonucleotides. *Nucleic Acids Res.*, **25**, 4264–4270.
5. Mann,M. and Dzau,V. (2000) Therapeutic applications of transcription factor decoy oligonucleotides. *J. Clin. Invest.*, **106**, 1071–1075.
6. Fell,P.L., Hudson,A.J., Reynolds,M.A., Usman,N. and Akhtar,S. (1997) Cellular uptake properties of a 2′-amino/2′-O-methyl-modified chimeric hammerhead ribozyme targeted to the epidermal growth factor receptor mRNA. *Antisense Nucleic Acid Drug Dev.*, **7**, 319–326.
7. Santiago,F.S., Lowe,H.C., Kavurma,M.M., Chesterman,C.N., Baker,A., Atkins,D.G. and Khachigian,L.M. (1999) New DNA enzyme targeting Egr-1 mRNA inhibits vascular smooth muscle proliferation and regrowth after injury. *Nature Med.*, **5**, 1264–1269.
8. Elbashir,S.M., Harborth,J., Lendeckel,W., Yalcin,A., Weber,K. and Tuschl,T. (2001) Duplexes of 21-nucleotide RNAs mediate RNA interference in cultured mammalian cells. *Nature*, **411**, 494–496.
9. Timmons,L. and Fire,A. (1998) Specific interference by ingested dsRNA. *Nature*, **395**, 854.
10. Bridonneau,P., Chang,Y.-F., O'Connell,D., Gill,S.C., Snyder,D.W., Johnson,L., Goodson,T.,Jr, Herron,D.K. and Parma,D.H. (1998) High-affinity aptamers selectively inhibit human nonpancreatic secretory phospholipase A_2 (hnps-PLA_2). *J. Med. Chem.*, **41**, 778–786.
11. Collin,D., van Heijenoort,C., Boiziau,C., Toulmé,J.-J. and Guittet,E. (2000) NMR characterization of a kissing complex formed between the TAR RNA element of HIV-1 and a DNA aptamer. *Nucleic Acids Res.*, **28**, 3386–3391.
12. Yoon,K., Cole-Strauss,A. and Kmiec,E.B. (1996) Targeted gene correction of episomal DNA in mammalian cells mediated by a chimeric RNA.DNA oligonucleotide. *Proc. Natl Acad. Sci. USA*, **93**, 2071–2076.
13. Schmajuk,G., Sierakowska,H. and Kole,R. (1999) Antisense oligonucleotides with different backbones. *J. Biol. Chem.*, **274**, 21783–21789.
14. Fisher,T.L., Terhorst,T., Cao,X. and Wagner,R.W. (1993) Intracellular disposition and metabolism of fluorescently-labeled unmodified and modified oligonucleotides microinjected into mammalian cells. *Nucleic Acids Res.*, **21**, 3857–3865.
15. Agrawal,S., Jiang,Z., Zaho,Q., Shaw,D., Cai,Q., Roskey,A., Channavajjala,L., Saxinger,C. and Zhang,R. (1997) Mixed-backbone oligonucleotides as second generation antisense oligonucleotides: *in vitro* and *in vivo* studies. *Proc. Natl Acad. Sci. USA*, **94**, 2620–2625.
16. Chin,D.J., Green,G.A., Zon,G., Szoka,F.C. and Straubinger,R.M. (1990) Rapid nuclear accumulation of injected oligodeoxyribonucleotides. *New. Biol.*, **2**, 1091–1100.
17. Leonetti,J.-P., Mechti,N., Degols,G., Gagnor,C. and Lebleu,B. (1991) Intracellular distribution of microinjected antisense oligonucleotides. *Proc. Natl Acad. Sci. USA*, **88**, 2702–2706.
18. Dokka,S. and Rojanasakul,Y. (2000) Novel non-endocytic delivery of antisense oligonucleotides. *Adv. Drug Deliv. Rev.*, **44**, 35–49.
19. Juliano,R.L. (2000) Aspects of the transport and delivery of antisense oligonucleotides. *Curr. Opin. Mol. Ther.*, **2**, 297–303.
20. Yakubov,L.A., Deeva,E.A., Zarytova,V.F., Ivanova,E.M., Ryte,A.S., Yurchenko,L.V. and Vlassov,V.V. (1989) Mechanism of oligonucleotide uptake by cells: involvement of specific receptors? *Proc. Natl Acad. Sci. USA*, **86**, 6454–6458.
21. Beltinger,C., Saragovi,H.U., Smith,R.M., LeSauteur,L., Shah,N., DeDionisio,L., Christensen,L., Raible,A., Jarett,L. and Gewirtz,A.M. (1995) Binding, uptake, and intracellular trafficking of phosphorothioate-modified oligodeoxynucleotides. *J. Clin. Invest.*, **95**, 1814–1823.
22. Laktionov,P.P., Dazard,J.-E., Vives,E., Rykova,E.Y., Piette,J., Vlassov,V.V. and Lebleu,B. (1999) Characterisation of membrane oligonucleotide-binding proteins and oligonucleotide uptake in keratinocytes. *Nucleic Acids Res.*, **27**, 2315–2324.
23. Zhu,F.-G., Reich,C.F. and Pisetsky,D.S. (2001) The role of macrophage scavenger receptor in immune stimulation by bacterial DNA and synthetic oligonucleotides. *Immunology*, **103**, 226–234.
24. Biessen,E.A.L., Vietsch,H., Kuiper,J., Bijsterbosch,M.K. and van Berkel,T.J.C. (1998) Liver uptake of phosphodiester oligodeoxynucleotides is mediated by scavenger receptors. *Mol. Pharmacol.*, **53**, 262–269.
25. Benimetskaya,L., Loike,J.D., Khaled,Z., Loike,G., Silverstein,S.C., Cao,L., El Khoury,J., Cai,T.-Q. and Stein,C.A. (1997) Mac-1 (CD11b/CD18) is an oligodeoxynucleotide-binding protein. *Nature Med.*, **3**, 414–420.
26. Biessen,E.A.L., Vietsch,H., Rump,E.T., Fluiter,K., Kuiper,J., Bijsterbosch,M.K. and van Berkel,T.J.C. (1999) Targeted delivery of oligodeoxynucleotides to parenchymal liver cells *in vivo*. *Biochem. J.*, **340**, 783–792.
27. Loke,S.L., Stein,C.A., Zhang,X.H., Mori,K., Nakanishi,M., Subasinghe,C., Cohen,J.S. and Neckers,L.M. (1989) Characterization of oligonucleotide transport into living cells. *Proc. Natl Acad. Sci. USA*, **86**, 3474–3478.
28. Hemmi,H., Takeuchi,O., Kawai,T., Kaisho,T., Sato,S., Sanjo,H., Matsumoto,M., Hoshino,K., Wagner,H., Takeda,K. and Akira,S. (2000) A toll-like receptor recognizes bacterial DNA. *Nature*, **408**, 740–745.
29. Yao,G.Q., Corrias,S. and Cheng,Y.C. (1996) Identification of two oligodeoxyribonucleotide binding proteins on plasma membranes of human cell lines. *Biochem. Pharmacol.*, **51**, 431–436.
30. de Diesbach,P., Berens,C., N'Kuli,F., Monsigny,M., Sonveaux,E., Wattiez,R. and Courtoy,P.J. (2000) Identification, purification and partial characterisation of an oligonucleotide receptor in membranes of HepG2 cells. *Nucleic Acids Res.*, **28**, 868–874.
31. Tonkinson,J.L. and Stein,C.A. (1994) Patterns of intracellular compartimentalization, trafficking and acidification of 5′-fluorescein labeled phosphodiester and phosphorothioate oligodeoxynucleotides in HL60 cells. *Nucleic Acids Res.*, **22**, 4268–4275.
32. Pichon,C. Arar,K., Stewart,A.J., Duc Dodon,M., Gazzolo,L., Courtoy,P.J., Mayer,R., Monsigny,M. and Roche,A.-C. (1997) Intracellular routing and inhibitory activity of oligonucleopeptides containing a KDEL motif. *Mol. Pharmacol.*, **51**, 431–438.
33. Aubert,Y., Bourgerie,S., Meunier,L., Mayer,R., Roche,A.C., Monsigny,M., Thuong,N.T. and Asseline,U. (2000) Optimized synthesis of phosphorothioate oligodeoxyribonucleotides substituted with a 5′-protected thiol function and a 3′-amino group. *Nucleic Acids Res.*, **28**, 818–825.
34. Berens,C., Courtoy,P.J. and Sonveaux,E. (1999) A fluorescent radioiodinated oligonucleotidic photoaffinity probe for protein labeling: synthesis and photolabeling of thrombin. *Bioconjug. Chem.*, **10**, 56–61.
35. Smith,P.K., Krohn,R.I., Hermanson,G.T., Mallia,A.K., Gartner,F.H., Provenzano,M.D., Fujimoto,E.K., Goeke,N.M., Olson,B.J. and Klenk,D.C. (1985) Measurement of protein using bicinchoninic acid. *Anal. Biochem.*, **150**, 76–85.
36. Steinman,R.M. and Cohn,Z.A. (1972) The interaction of soluble horseradish peroxidase with mouse peritoneal macrophages *in vitro*. *J. Cell Biol.*, **55**, 186–204.

37. Barrett,A.J. (1976) An improved color reagent for use in Barrett's assay of cathepsin B. *Anal. Biochem.*, **76**, 374–376.
38. Brightwell,R. and Tappel,A.L. (1968) Subcellular distribution and properties of rat liver phosphodiesterases. *Arch. Biochem. Biophys.*, **124**, 325–332.
39. Leighton,F., Poole,B., Beaufay,H., Baudhuin,P., Coffey,J.W., Fowler,S. and de Duve,C. (1968) The large-scale separation of peroxisomes, mitochondria and lysosomes from the livers of rats injected with Triton WR-1339. Improved isolation procedures, automated analysis, biochemical and morphological properties of fractions. *J. Cell Biol.*, **37**, 482–513.
40. Beck,G.F., Irwin,W.J., Nicklin,P.L. and Akhtar,S. (1996) Interactions of phosphodiester and phosphorothioate oligonucleotides with intestinal epithelial caco-2 cells. *Pharm. Res.*, **13**, 1028–1037.
41. Geselowitz,D.A. and Neckers,L.M. (1995) Bovine serum albumin is a major oligonucleotide-binding protein found on the surface of cultured cells. *Antisense Res. Dev.*, **5**, 213–217.
42. Gonzalez-Noriega,A., Grubb,J.H., Talkad,V. and Sly,W.S. (1980) Chloroquine inhibits lysosomal enzyme pinocytosis and enhances lysosomal enzyme secretion by impairing receptor recycling. *J. Cell Biol.*, **85**, 839–852.
43. de Duve,C., de Barsy,T., Poole,B., Trouet,A., Tulkens,P. and Van Hoof,F. (1974) Lysosomotropic agents. *Biochem. Pharmacol.*, **23**, 2495–2531.
44. Limet,J.N., Quintart,J., Schneider,Y.-J. and Courtoy,P.J. (1985) Receptor-mediated endocytosis of polymeric IgA and galactosylated serum albumin in rat liver. Evidence for intracellular ligand sorting and identification of distinct endosomal compartments. *Eur. J. Biochem.*, **146**, 539–548.
45. Nakai,D., Seita,T., Terasaki,T., Iwasa,S., Shoji,Y., Mizushima,Y. and Sugiyama,Y. (1996) Cellular uptake mechanism for oligonucleotides: involvement of endocytosis in the uptake of phosphodiester oligonucleotides by a human colorectal adenocarcinoma cell line, HCT-15. *J. Pharmacol. Exp. Ther.*, **278**, 1362–1372.
46. Berthiaume,E.P., Medina,C. and Swanson,J.A. (1995) Molecular size-fractionation during endocytosis in macrophages. *J. Cell Biol.*, **129**, 989–998.
47. Haller,T., Ortmayr,J., Friedrich,F., Völki,H. and Dietl,P. (1998) Dynamics of surfactant release in alveolar type II cells. *Proc. Natl Acad. Sci. USA*, **95**, 1579–1584.
48. Wiley,H.S. and Cunningham,D.D. (1982) The endocytotic rate constant. A cellular parameter for quantitating receptor-mediated endocytosis. *J. Biol. Chem.*, **257**, 4222–4229.
49. Hansen,S.H., Sandvig,K. and van Deurs,B. (1992) Internalization efficiency of the transferrin receptor. *Exp. Cell Res.*, **199**, 19–28.
50. Dörner,M., Altmann,M., Pääbo,S. and Mörl,M. (2001) Evidence for import of a lysyl-tRNA into marsupial mitochondria. *Mol. Biol. Cell*, **12**, 2688–2698.
51. Pichon,C., Monsigny,M. and Roche,A.-C. (1999) Intracellular localization of oligonucleotides: influence of fixative protocols. *Antisense Nucleic Acids Drug Dev.*, **9**, 89–93.